

PAPER

## On similarity scaling of tokamak fusion plasmas with different aspect ratio

To cite this article: Michele Romanelli and Francesco Paolo Orsitto 2021 *Plasma Phys. Control. Fusion* **63** 125004

View the [article online](#) for updates and enhancements.

### You may also like

- [The effective modulus of super carbon nanotubes predicted by molecular structure mechanics](#)  
Ying Li, XinMing Qiu, Fan Yang et al.
- [Bontomarannu Education Park Reviewed from Conservation, Social, and Environmental Aspects](#)  
Rismawati, Syahribulan and Slamet Santosa
- [The spherical tokamak programme at Culham](#)  
A. Sykes, the START Team, the NBI Team et al.



**IOP | ebooks™**

Bringing together innovative digital publishing with leading authors from the global scientific community.

Start exploring the collection—download the first chapter of every title for free.

# On similarity scaling of tokamak fusion plasmas with different aspect ratio

Michele Romanelli\*  and Francesco Paolo Orsitto 

Tokamak Energy Ltd, 173 Brook Drive, Milton Park, Oxfordshire OX14 4SD, United Kingdom

E-mail: [Michele.Romanelli@tokamakenergy.co.uk](mailto:Michele.Romanelli@tokamakenergy.co.uk)

Received 16 April 2021, revised 24 August 2021

Accepted for publication 3 September 2021

Published 21 October 2021



CrossMark

## Abstract

Previously, tokamak research has been focused mainly on large aspect ratio devices where the vessel/plasma major radius is about a factor three larger than the plasma radius. This research culminated in the design and construction of the international thermonuclear experimental reactor, ITER. Spherical tokamaks (ST), with aspect ratio below two, represent an attractive alternative to large aspect ratio tokamaks as, in our opinion, provide a faster, more economical and compact solution on the path to a fusion reactor. STs are the focus of research at Tokamak Energy Ltd with its present device ST40 in operation and the first ST reactor being designed, taking advantage of the high temperature superconductor (HTS) technology. HTS allow to design a ST with magnetic field/comparable or exceeding that of present-day large aspect ratio tokamaks. However, plasma studies carried out so far on compact, low aspect ratio tokamaks have been limited to small, low magnetic field, low plasma-current devices and therefore the data available for extrapolating to large scale ST plasmas is limited. This paper addresses the problem of scaling the results of large aspect ratio tokamak and existing ST plasmas to a high field ST reactor using plasma-similarity arguments in order to mitigate its design and operational risks. The role of the plasma aspect ratio in scaling burning plasmas as well as conventional experiments in deuterium is highlighted. We find that the scaling for fusion-reactor plasmas exhibit a stronger dependence on the magnetic field and aspect ratio than the one of conventional non-burning plasmas. The parameters of a ST having the same fusion gain  $Q_{\text{fus}}$  of ITER under different confinement assumptions and for different aspect ratios are presented and discussed.

Keywords: similarity, scaling, tokamak, fusion, plasmas, aspect-ratio

(Some figures may appear in colour only in the online journal)

## 1. Introduction

Spherical tokamaks (STs) are typically defined as tokamaks having aspect ratio (ratio between the plasma major and minor radius) less than 2 and are characterized by a strong variation of the toroidal magnetic field from high to low field side [1]. The largest STs which have operated or will be soon in operation at the time of writing are NSTX/NSTX-U [2] and MAST/MAST-U [3]. The ST presently in operation at Tokamak Energy Ltd is ST40 [4] which has an aspect ratio of

1.6–1.8, toroidal magnetic field up to 3 T and plasma current up to 2 MA. STs have been identified as complementary to the conventional line of research represented by international thermonuclear experimental reactor (ITER) and the demonstration reactor (DEMO). Their attractiveness stems from the compact size, improved confinement, high-beta, possibility of continuous operation and reduced construction costs, which can translate in reduced cost of electricity [5]. At the time of writing the experimental database on ST plasmas is limited to magnetic-fields not exceeding 0.55 T, plasma currents less than 1.4 MA, major radius less than 1 m and there are therefore large uncertainties when extrapolating performances to the high field (4–5 T), high current (10–13 MA), larger (>2 m)

\* Author to whom any correspondence should be addressed.

versions envisaged for an ST fusion power plant. However, the magnetic field, plasma current and size of an ST reactor with a fusion gain factor well above 1 are expected to be close to those of present-large aspect ratio tokamaks ( $B = 3\text{--}4$  T and  $I_p = 5$  MA). Therefore, the question arises on whether results from present day tokamaks can be used to fill the gap on ST research and be projected to low aspect ratio devices at similar magnetic field and current. To answer this question, we will use the concept of plasma similarity first introduced by Kadomtsev [6]. The matching of dimensionless plasma parameters is often used in fusion research to perform similarity experiments in different tokamaks and to extrapolate scenarios from existing to planned tokamak devices. The aspect ratio  $A$  is one of the independent dimensionless parameters characterizing the plasma dynamics, however a detailed and focused analysis of plasma-scaling with  $A$  was so far missing in the literature. The focus of this paper is the identification of the dependence of the dimensional plasma parameters such as magnetic field, plasma current, plasma major radius on the aspect ratio both in conventional non-burning (hydrogen/deuterium) and burning (deuterium + tritium, DT) plasmas with same global confinement and/or same fusion gain factor and heating power, using dimensionless parameters to relate tokamaks of different scales. Plasma invariance as first described by Kadomtsev was derived under the hypothesis that alpha particle and atomic physics effects are negligible (valid for non-burning plasmas): this is not the case in burning plasmas where most of the heating comes from fusion reactions and alpha particle effects are dominant; taking this into account leads to the conclusion that similar burning plasmas do not necessarily operate at same dimensionless parameters. The paper is organized as follows: in section 2 the scaling of plasma dimensional parameters with aspect ratio is derived for conventional non-burning plasmas with same global confinement, in section 3 physics-based scaling laws for fusion reactors are derived; the main results are discussed in section 4. In particular: the similarity parameters obtained are used to determine an ITER similar plasma at low aspect ratio and high magnetic field; finally, section 5 reports the conclusions. The detailed derivation of the scaling of parameters for burning plasmas is reported in appendix A while the scaling of the dimensional plasma parameters for a non-burning plasma is derived in appendix B.

## 2. Derivation of the scaling of plasma parameters with aspect ratio for non-burning plasmas

### 2.1. Dimensional parameters of plasmas with same confinement

Following the reasoning in [6–12] we will assume that, for a non-burning plasma, the global energy-confinement is proportional to a function of normalized beta, collisionality, normalized ion Larmor radius and safety factor. It is then possible to consider confinement-similarity experiments between different tokamaks where the dimensionless parameters are held constant (along with any constant of proportionality) and write explicitly the scaling of the plasmas dimensional-variables such as plasma density  $n$ , plasma temperature  $T$ ,

**Table 1.** Scaling of dimensional parameters with aspect ratio  $A$ , isotopic mass  $M$  and major radius  $R$  for non-burning plasmas with same energy confinement.

Bulk plasma similarity: constant ( $q, \rho_{iT}^*, \nu^*, \beta_T, f$ ).	
$n \sim M R^{-2} A^2$	$ka \sim f(M, A)$
$T \sim M^{1/2} R^{-1/2} A^{7/4}$	$P_{\text{aux}} \sim \tau_E^{-1}$
$I_p \sim S M^{3/4} R^{-1/4} A^{-1/8}$	
$B \sim M^{3/4} R^{-5/4} A^{15/8}$	

plasma current  $I_p$ , magnetic field  $B$  and input auxiliary power  $P_{\text{aux}}$  with aspect ratio  $A$ , ion mass  $M$  and major radius  $R$ , using the definitions of the plasma dimensionless parameters:

$$A = \frac{R}{a}; \beta_T \propto \frac{nT}{B^2}; \beta_P \propto \frac{nT}{I_p^2}; \rho_{iT} \propto \frac{(MT)^{1/2}}{aB}; \rho_{iP} \propto \frac{(MT)^{1/2}}{I_p};$$

$$q \propto \frac{RB}{A^2 I_p}; \nu^* \propto nRqT^{-2}A^{3/2},$$

where  $\beta_T$  is the toroidal beta,  $\beta_P$  is the poloidal beta  $\rho_{iT}$ ,  $\rho_{iP}$  are the normalized toroidal and poloidal ion Larmor radius respectively,  $q$  is the safety factor, where we have assumed plasma shaping equals to 1 (see discussion on shaping at the end of this section), and  $\nu^*$  the collisionality. The scaling of the dimensional plasma-variables with  $A$ ,  $M$ ,  $R$  and  $B$  calculated using the above definitions of the dimensionless-parameters is summarized in table 1. The additional dimensionless parameter  $f$  in table 1 is the product of all the factors that appear in empirical confinement-time scaling related to plasma geometry and plasma composition (typically  $f = f(ka, A, M)$  with  $ka$  being the plasma elongation) and needs to be the same for plasmas with same confinement. The exact form of  $f$  depends on the confinement scaling and will be discussed in the next section. Detailed derivation of the scaling is reported in appendix B.

It is important to notice that: (a) the scaling in table 1 are ‘engineering’ expressions of the realization of similar bulk-plasmas having the same dimensionless-parameters and hence same confinement.

(b) The scaling derived in table 1 is valid for any functional dependence of the energy confinement time on the dimensionless parameters: normalized beta, collisionality, normalized ion Larmor radius and safety factor.

A similarity function,  $S_K$  characterizing the dependence on  $B$ ,  $A$ ,  $M$ ,  $R$  of a family of tokamak plasmas equivalent in terms of energy confinement can be easily constructed by taking the expression for the scaling of the magnetic field from table 1 and writing the ratio of the left-hand side to the right-hand side terms as a dimensional constant:

$$B \sim M^{3/4} R^{-5/4} A^{15/8}$$

$$BM^{-3/4} R^{5/4} A^{-15/8} = \text{constant}.$$

By elevating the above expression to the power 4/5 we obtain the desired function  $S_K$ :

$$S_K = RB^{4/5} A^{-3/2} M^{-3/5}.$$

Any choice of  $R$ ,  $B$ ,  $A$ ,  $M$  that gives the same value of  $S_K$  will lead to plasmas with the same confinement as long as the function  $f$  is also conserved.

The  $S_K$  function indicates that, by going from high to low aspect ratio all the plasma dimensional parameters must be decreased (only the plasma current  $I_p$  remains nearly constant, see table 1.): the magnetic field must be decreased by  $\Delta B/B = -18.7\%$  for a reduction of the aspect ratio of  $\Delta A/A = -10\%$ . A device with low aspect ratio ( $A < 2$ ) operating at the same ( $q$ ,  $\rho^*$ ,  $\nu^*$ ,  $\beta_T$ ,  $f$ ) values of a device at large aspect ratio ( $A = 3$ ), will require a substantially lower magnetic field.

In highly-shaped, low aspect ratio devices, plasma elongation is an important parameter, and can be included in the scaling. It is easy to show that elongation will impact only the scaling of the plasma current. Introducing the shaping factor  $S = (1 + ka^2)/2$ , the safety factor  $q$  can be written as [13]:

$$q \sim \frac{R B (1 + ka^2)}{I_p A^2}.$$

We can then write the scaling of the current with elongation as:

$$I_p \sim R^{-1/4} M^{3/4} A^{-1/8} \frac{(1 + ka^2)}{2}.$$

The scaling with  $A$ ,  $M$ ,  $R$  of the elongation and of the heating-power  $P_{\text{aux}}$  necessary to achieve the same energy confinement require specifying the dependency of the energy confinement time on the engineering parameters and will be derived in the next section.

## 2.2. Scaling of heating power for confinement-similarity experiments

The dependency of the heating power on  $R$ ,  $A$ ,  $M$  can be obtained by specifying the scaling-law of the energy confinement: here we shall consider the IPB(y,2), the ITPA20 and the NSTX extended scaling [14–16] respectively. The NSTX extended scaling has been derived using the NSTX confinement database while IPB(y,2) and ITPA20 arise from the analysis of ELMy H-mode pulses (high confinement plasmas characterized by edge localized modes) of the multi tokamak international database: the ITPA20 database also includes data from START, MAST and NSTX. IPB(y,2) and ITPA20 provide the same dependency of the confinement time on the dimensional plasma parameters, however, the dependency on the dimensionless parameters differs [16]. The scaling in ITPA20 with collisionality and safety factor is compatible with the one found in the NSTX extended scaling.

The expressions taken as reference in this paper are (where only the main dependences from the plasma quantities are reported):

$$\tau_{\text{IPB}(y,2)/\text{ITPA20}} = 0.13 I_p P_{\text{loss}}^{-0.69} n^{0.40} R^{2.00} B^{0.20} f_{\text{ITER}}(A, M, ka) \quad (1)$$

$$\tau_{\text{NSTX}} = 0.21 I_p^{0.54} P_{\text{loss}}^{-0.38} n^{-0.05} R^{2.14} B^{0.91} f_{\text{NSTX}}(A, M, ka). \quad (2)$$

The power in equations (1) and (2) is the  $P_{\text{loss}}$  (power flowing from the plasma core to the scrape off layer, in units of MW as defined in [15, 16]), the other units are:  $I_p$  [MA],  $R$  [m],  $M$  dimensionless ion mass, the ion mass in atomic mass units ( $M = \text{ion mass/hydrogen mass}$ ),  $n$  [in units of  $10^{19} \text{ m}^{-3}$ ],  $B$  [T] the magnetic field. In particular equation (1) corresponds to equation (5) in [15] and equation (7) in [16] for  $f_{\text{ITER}}(A, M, ka) = A^{-0.60} M^{0.20} ka^{0.80}$ , while equation (2) corresponds to equation (12) in [15] when  $f_{\text{NSTX}}(A, M, ka) = 1$ . The NSTX extended scaling has been derived from NSTX experimental data at  $\langle A \rangle = 1.45$ ,  $M = 2$  and therefore cannot provide ion mass and aspect ratio dependence of confinement time. Also, the variation in  $ka$  is very limited in the database and does not allow to identify a scaling with elongation either. In this paper we shall use the NSTX scaling only to highlight the differences with IPB(y,2)/ITPA20 when extrapolating to a spherical-tokamak reactor with NSTX aspect ratio.

We notice here that the ITPA20 scaling has been derived using data of STs and therefore applies to a wider range of aspect ratios than the IPB(y,2) scaling, including  $A < 2$ , even if the exponents are different than those of the NSTX scaling. Indeed, the transport in STs and conventional tokamaks is caused in both cases by drift wave instabilities described by e.g. gyrokinetic theory, the main difference, along with parallel magnetic field variation and high  $q$ , magnetic shear stabilizations, is that they typically operate at different beta and collisionality and therefore the dominant unstable modes are different, leading to different turbulence regime and scaling of confinement.

In terms of dimensionless parameters the scaling laws are given by the following expressions:

$$\Omega_{ci} * \tau_{\text{IPB}(y,2)} \sim \rho^{*-2.70} \beta_T^{-0.90} \nu^{*-0.01} M^{0.96} q^{-3.00} A^{-0.73} ka^{2.30}. \quad (1')$$

$$\Omega_{ci} * \tau_{\text{NSTX}} (A = 1.45) \sim \rho^{*-3.00} \beta_T^{-0.17} \nu^{*-0.53} q^{-0.35}. \quad (2')$$

$$\Omega_{ci} * \tau_{\text{ITPA20}} \sim \rho^{*-2.24} \beta_T^{0.20} \nu^{*-0.47} M^{0.53} q^{-0.70} A^{1.70} ka^{0.54}. \quad (3')$$

Equation (1') corresponds to equation (6) and to equation (21) in the ITER Physics Basis [14], while equation (2') to equation (12) in [15], equation (3') is equation (8) in [16]. Equations (1') and (3') include the complete dependence on the ion mass (see also [14] equation (21)). In the context of the scaling laws for plasma confinement, specific analysis was carried out to include ST data (NSTX, MAST, START) in the ITER database [17–20, 16–18] to reveal additional dependence of the confinement on the aspect ratio. The conclusion was that the dependency on the aspect ratio included in the ITER IPB(y,2) scaling is compatible with the available ST data [16]. The scaling of the additional heating for plasma similarity can be obtained noting that (see section 1)  $P_{\text{loss}} = \text{total plasma energy}(W_{\text{th}})/\text{confinement time}(\tau_E) \sim P_{\text{aux}}$ . Inserting the expressions given in table 1, which assume confinement time depending only on  $\rho^*$ ,  $\beta$ ,  $\nu^*$ ,  $q$ , and using the formula  $P_{\text{loss}} = W_{\text{th}}/\tau_E \sim n T R^3 A^{-2} ka/\tau_E$  (where  $R^3 A^{-2} ka$  is the

plasma volume), we get the following scaling for the heating power:

$$P_{\text{aux IPB}(y,2)} \sim R^{-0.78} A^{3.58} M^{0.29} \text{ka}^{0.71} S^{-3.00} f_{\text{ITER}}(A, M, \text{ka})$$

$$= \text{const} \quad (3)$$

$$P_{\text{aux NSTX}} \sim R^{-0.75} A^{0.33} M^{0.76} \text{ka}^{1.61} S^{-0.87} \sim R^{-0.75}$$

$$A = 1.45, M = 2, \text{ka} = \text{ka}_{\text{NSTX}}. \quad (4)$$

Equation (3) is valid when the additional dimensionless parameter  $f_{\text{ITER}}(A, M, \text{ka}) = \text{const}$ , in accordance to our hypothesis of section 2.1 that for similar plasmas, confinement depends only on  $\rho^*$ ,  $\beta$ ,  $\nu^*$ ,  $q$  and  $f$ . In other words, the choice of  $\text{ka}$  in two similar plasmas for given  $A$  and  $M$  has to be such that  $f$  is constant. Inspecting equations (3) and (4) we see that the dependence of  $P_{\text{aux NSTX}}$  on the major radius is similar to  $P_{\text{aux IPB}(y,2)}$ .

In table 2 we report the parameters of a set of ST40-confinement-similarity experiments that could be conducted in various large aspect ratio devices.

### 3. Derivation of the scaling of plasma parameters with aspect ratio of reactor class plasmas

Plasma similarity via the identity of dimensionless parameters as discussed in the previous section does not apply to burning plasmas where the DT fusion reaction-rate plays a crucial role. We need therefore to define similarity in terms of a different set of assumptions. The extension of the methodology outlined in the previous sections to burning plasmas [12] will need the introduction of the alpha particle power ( $P_\alpha$ ) in the power balance as dominant heating; the gain factor  $Q$  and the alpha (classical) slowing down time  $\tau_{\text{SD}}$  as parameters defining the plasma state.  $P_\alpha$  is the energy transferred by the alpha particles to the thermal plasma per unit time;  $Q$  is the triple product  $nT\tau_{\text{E}}$  function of the fusion gain  $Q_{\text{fus}}$  defined as the ratio between fusion power and external heating (see appendix A for the relation between  $Q$  and  $Q_{\text{fus}}$ );  $\tau_{\text{SD}}$  is the time for alpha particles to thermalize with the rest of the plasma via collisions to thermal electrons and ions. The parameters specific of the alpha particle physics related to the ion transport and interaction with magneto hydro dynamic modes and turbulence are  $\beta_\alpha \sim n_\alpha E_\alpha/B^2$ , and the ratio  $V_\alpha/V_{\text{Alfven}}$ .

In this paper we shall consider the following set of conditions to define burning plasma similarity:

$$Q = Q_0, \tau_{\text{SD}}/\tau_{\text{E}} = \Lambda_{\text{SD}} (\Lambda_{\text{SD}} \ll 1),$$

$$P_\alpha/P_{\text{LH}} = \Lambda_{\text{th}} (\Lambda_{\text{th}} > 1.5 \text{ for H-mode}),$$

where  $\tau_{\text{SD}}$  is the slowing-down time of alpha particles,  $\tau_{\text{E}}$  is the confinement time,  $P_{\text{LH}}$  the L-H threshold power (power necessary to transit into H-mode confinement), and  $Q_0$ ,  $\Lambda_{\text{SD}}$  and  $\Lambda_{\text{th}}$  are constants.

The above set of conditions define a reactor plasma that works in H-mode, with triple product  $Q_0$ , dominant alpha heating, and alpha power well above the L-H transition power

threshold in order to sustain the high confinement mode. It is important to note that the above choice of conditions is not the only possible choice and a different definition of burning plasma similarity conditions would lead to a different scaling.

The condition  $\tau_{\text{SD}}/\tau_{\text{E}} = \Lambda_{\text{SD}}$  ( $\Lambda_{\text{SD}} \ll 1$ ) is consistent with the usual assumption that the alpha particle beta ( $\beta_\alpha$ ) must be smaller than the total plasma beta. This is shown below (where  $n_\alpha$ ,  $E_\alpha$ ,  $P_\alpha$ , are the alpha particle density, energy, and power respectively).

$\beta_\alpha < \beta$  can be written as  $n_\alpha E_\alpha/B^2 < nT/B^2$ . By using  $n_\alpha E_\alpha \sim P_\alpha \tau_{\text{SD}}$  and  $nT \sim P_{\text{loss}} \tau_{\text{E}}$ , from the condition  $P_\alpha \sim P_{\text{loss}}$ , we obtain  $\tau_{\text{SD}} < \tau_{\text{E}}$ .

The main difference with the plasma similarity scaling derived in section 1 is that, in order to make use of the set of conditions for a burning plasma we need to specify *a priori* the scaling of confinement with engineering parameters. The detailed calculation is reported in appendix A where three energy confinement-time scaling are considered, IPB(y,2), ITPA20 and NSTX. It is important to notice that although the confinement-scaling above have been derived for non-burning plasmas, so far, we do not have any experimental evidence that they do not apply to burning plasmas: the confinement times observed in the first JET DT (deuterium–tritium) campaign in 1997, providing the most recent study of fusion plasmas with some additional alpha heating, have been found to be consistent with the ITER scaling. The result of appendix A is that depending on the scaling of confinement-time, the plasma major radius for similar burning plasmas has the following dependency on the plasma engineering parameters (where  $R_{\text{ITER}}$  is derived with the IPB(y,2) scaling,  $R_{\text{ST}}$  is derived with the NSTX extended scaling and  $R_{\text{ITPA20}}$  with the ITPA20 scaling):

$$R_{\text{ITER}} = C_{\text{ITER}} H_{y2}^{-1/2.62} B^{-1.36} Q_0^{0.59} \text{ka}^{-0.88} A^{1.28} M^{-0.23} q^{1.15}$$

$$C_{\text{ITER}} = \left( \frac{\Lambda_{\text{SD}}}{A_{\text{SD}}} \right)^{-0.55} \left( \frac{\Lambda_{\text{th}} A_{\text{th}}}{f_\alpha} \right)^{0.07} C_{\tau y2} \quad (5)$$

$$R_{\text{ST}} = C_{\text{ST}} H_{\text{ST}}^{-1/2.23} Q_0^{0.46} B^{-1.13} A^{1.59} M^{0.22} q^{0.4}$$

$$C_{\text{ST}} = \left( \frac{\Lambda_{\text{SD}}}{A_{\text{SD}}} \right)^{-0.04} \left( \frac{\Lambda_{\text{th}} A_{\text{th}}}{f_\alpha} \right)^{0.24} C_{\tau \text{ST}} \quad (5')$$

$$R_{\text{ITPA20}} = C_{20} H_{\text{ITPA}}^{-1/1.19} M^{-0.34} A^{0.55} \text{ka}^{0.54} B^{-1.02} Q_0^{0.89} q^{0.98}. \quad (5'')$$

In equations (5), (5'), (5'')  $C_{\text{ITER}}$ ,  $C_{\text{ST}}$  and  $C_{20}$  are dimensional-constants, where  $H$  is the ratio of the actual to the scaled confinement time. The expressions in equation (5') are obtained using the NSTX extended confinement scaling and are valid for aspect ratio and elongation equal to that of NSTX only. From equation (5), (5'), (5'') we obtain similarity parameters to compare with that obtained for non-burning plasmas in section 2. The similarity parameters

**Table 2.** Parameters of large aspect ratio plasmas for similarity experiments with ST40. The definition of the parameters is given in this section,  $q$  is the safety factor that appears in the confinement scaling 1', 2', 3' (typically defined as the value at 95% of the plasma minor radius).

	ST40	JET	DIII-D	JT-60SA
$S_K$	0.54	0.54	0.54	0.54
$F$	0.17	0.17	0.17	0.17
$R$ (m)	0.50	3.00	1.67	2.96
$B$ (T)	2.67	1.55	2.30	1.12
$A$	1.60	3.00	2.50	2.50
$M$	1.00	2.00	2.00	2.00
$Q$	8.00	8.00	8.00	8.00
ka	1.82	2.00	2.15	2.15
$n$ ( $10^{20} \text{ m}^{-3}$ )	1.00	0.19	0.43	0.14
$I_p$ (MA)	1.00	0.40	0.15	0.15
$T$ (keV)	3.00	5.20	5.06	3.80
$P_{\text{aux IPB}(y,2)}$ (MW)	0.70	3.70	2.30	1.60
$P_{\text{aux NSTX}}$ (MW)	0.70	0.30	0.50	0.30

for fusion reactors, depending on the confinement scaling, are:

$$\begin{aligned}
 S_{\text{FR}} &= C'_{\text{ITER}} H_{y2}^{1/2.62} R_{\text{ITER}} B^{1.36} Q_0^{-0.59} \text{ka}^{0.88} A^{-1.28} \\
 &\quad M^{0.23} q^{-1.15} \\
 S_{\text{ST}} &= C_{\text{ST}}' H_{\text{ST}}^{1/2.23} R_{\text{ST}} Q_0^{-0.61} B^{1.13} A^{-1.59} M^{-0.22} q^{-0.4} \\
 S_{\text{ITPA20}} &= C_{20}' H_{\text{ITPA}}^{1/1.19} R_{\text{ITPA20}} M^{0.34} A^{-0.55} \text{ka}^{-0.54} B^{1.02} \\
 &\quad Q_0^{-0.89} q^{-0.98}.
 \end{aligned} \tag{6}$$

The conditions for burning plasma similarity, lead to a dependence on the magnetic field in the similarity parameter  $S_{\text{FR}}$ , stronger than in  $S_K$  (non-burning plasmas). Since the similarity parameter is proportional to the value  $Q_0$ , the major radius scales with magnetic field and aspect ratio as  $R \sim B^{-7/5} A^{5/4}$ .

From equations (5) and (5') we find a slow dependence of the gain factor on the major radius  $Q_0 \approx R^{5/8}$  that agrees with the formulas reported in [21]. However, equation (5) implies a stronger dependence on the magnetic field and aspect ratio, than in [21].

## 4. Discussion

### 4.1. Summary of scaling parameters and review of ITER class devices

In this section we summarize the main results of the previous sections, and we use the scaling parameters derived there to define a set of 'ITER-like' devices at different aspect ratio and magnetic field.

The first point to be noted is that the Kadomtsev similarity parameter for non-burning plasma derived in section 2.1 (see also table 1):

$$S_K = RB^{0.8} M^{-0.6} A^{-1.5}, \tag{7}$$

must be replaced in the context of fusion reactors by the scaling derived in section 3 (see section 3 equation (5)

and appendix A equation (A1.22)) leading to the following expressions:

$$\begin{aligned}
 R_{\text{ITER}} &= C_{\text{ITER}} H_{y2}^{-1/2.62} B^{-1.36} Q_0^{0.59} \text{ka}^{-0.88} A^{1.28} M^{-0.23} q^{1.15} \\
 C_{\text{ITER}} &= \left( \frac{\Lambda_{\text{SD}}}{A_{\text{SD}}} \right)^{-0.55} \left( \frac{\Lambda_{\text{th}} A_{\text{th}}}{f_{\alpha}} \right)^{0.07} C_{\tau y2}
 \end{aligned} \tag{8}$$

$$\begin{aligned}
 R_{\text{ST}} &= C_{\text{ST}} H_{\text{ST}}^{-1/2.23} Q_0^{0.46} B^{-1.13} A^{1.59} M^{0.22} q^{0.4} \\
 C_{\text{ST}} &= \left( \frac{\Lambda_{\text{SD}}}{A_{\text{SD}}} \right)^{-0.04} \left( \frac{\Lambda_{\text{th}} A_{\text{th}}}{f_{\alpha}} \right)^{0.24} C_{\tau \text{ST}}
 \end{aligned} \tag{9}$$

In equations (8) and (9), the aspect ratio can be considered an additional free parameter for the design and optimization of a fusion reactor.

For example, the major radius of a tokamak operating at  $B = 6.5$  T and  $A = 2.5$  having the same bulk-plasma performance of ITER (whose engineering parameters are  $R = 6.2$  m,  $B = 5.2$  T,  $A = 3.1$ ,  $M = 2.5$ ), will have a major radius (substituting in equations (7) and (8))  $R_{\text{ITER}} = 3.40$  m, which is smaller than  $R_K = 3.756$  m, where  $R_K$  is the major radius obtained using the scaling of equation (7) for non-burning plasmas,  $R_{\text{ITER}}$  that obtained using the scaling for fusion reactors (equation (8)). Following the results of the scaling for fusion reactors, a device with major radius  $R_{\text{ITER}} = 3.40$  m i.e. 19.5% larger than JT-60SA (whose parameters are  $R = 2.9$  m,  $B = 2.5$  T,  $A = 2.5$ ), with a magnetic field 2.6 times higher than JT-60SA would be a more compact reactor with same plasma performance as ITER.

### 4.2. Parameters of $Q_{\text{fus}} = 10$ ITER-like plasmas at different aspect ratio

Using equations (8) and (9) we can determine the major radius of ITER-like tokamaks at different aspect ratios: in this case the ITER parameters are taken as reference (see [6]), and the parameters of devices with bulk plasma similar to ITER

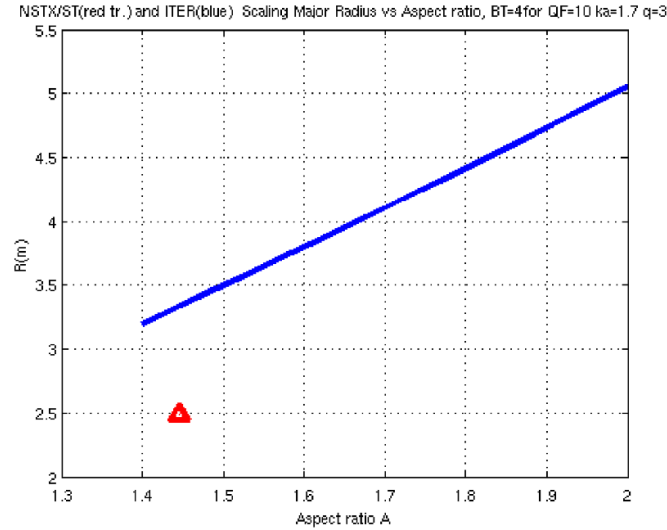


**Figure 1.** Major radius vs aspect ratio for STs at  $B = 4$  T evaluated using the IPB(y,2) confinement scaling and  $H_{y2} = 1$  (blue) and the NSTX extended scaling (red triangle). The NSTX extended confinement-time scaling does not contain an explicit dependence on aspect ratio, atomic mass and elongation.

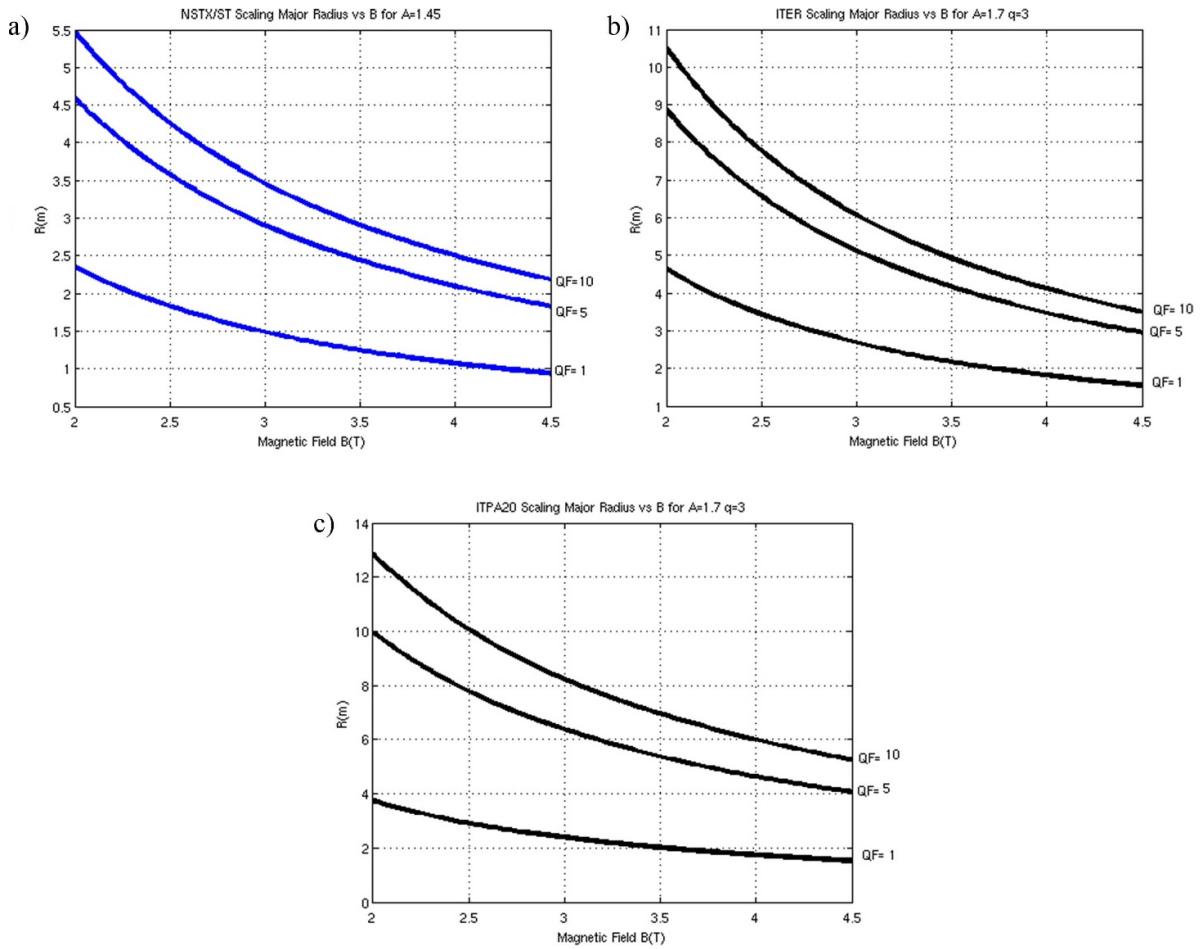


**Figure 2.** (a) Major radius vs magnetic field for ST reactors of aspect ratio  $A = 1.45$  (left) and (b)  $A = 1.7$  (right) for  $Q_{fus} = 1, 5, 10$ , respectively,  $H_{y2} = 1$ . As an example, using the scaling derived in appendix A, the working point at  $Q_{fus} = 10$ ,  $B = 3.5$  T,  $R = 2.89$  m,  $A = 1.45$  corresponds to a  $P_{fus} = 100$  MW,  $T = 20$  keV,  $\beta_N = 2.5$ ,  $q = 3$ ,  $I_p = 15$  MA, ITER similar plasma. (c)  $R$  vs  $B$  using the ITPA20 scaling for a device with  $A = 1.7$ , at various  $Q_{fus} = 1, 5, 10$  and  $H_{y2} = 1$ .

$Q_{\text{fus}} = 10$  are obtained by using the similarity parameter  $S_{\text{FR/ST}}$ , figure 1. The scaling of major radius with toroidal magnetic field for tokamaks having aspect ratio  $A = 1.45$ ,  $A = 1.7$  and  $Q_{\text{fus}} = 1, 5, 10$  is shown in figure 2.

According to figure 1, plasma major radius increases by 60% when the aspect ratio increases from  $A = 1.4$  to  $A = 2$ . In practice, this increase will translate in larger toroidal field coils, the size of which will depend not only on the major radius but also on plasma elongation. To quantify the impact of the increase of plasma major radius on the cost of the tokamak, it is useful to use the plasma perimeter instead of the major radius since the cost of the device is determined in large portion by the cost of the toroidal field coils: in this case the perimeter (and hence the cost) increases by only 20% when increasing the aspect ratio from  $A = 1.4$  to  $A = 2$ .

## 5. Conclusions

The role of the aspect ratio when designing similarity experiments between conventional and STs has been studied in the case of non-burning and burning plasma experiments. The investigation is motivated by the increasing importance of STs in the context of fusion energy production and the need to extrapolate results from the widely studied conventional aspect ratio tokamaks for use in the design of a ST reactor. By introducing the aspect ratio as one of the dimensionless parameters in the Kadomtsev similarity scheme, it was possible to derive a complete set of similarity scaling for non-burning plasmas including the scaling with aspect ratio of the toroidal magnetic field, plasma density, plasma temperature and plasma current. The assumption for the above derivation is that two similar non-burning plasmas operate at constant dimensionless parameters  $\rho^*$ ,  $\beta$ ,  $\nu^*$  safety factor  $q$  and that the plasma elongation compensates for the different aspect ratio and isotopic mass dependence in the confinement time scaling. With the above hypothesis, we find that there is strong sensitivity of the plasma engineering parameters on the aspect ratio as shown in table 1. The parameters of similarity experiments between ST40 and other tokamaks are reported in table 2. The above table should guide and stimulate the execution of ST relevant similarity experiments in conventional tokamaks. The interest of these experiments for the ST community is that they will provide data bridging the gap between STs and conventional tokamaks and will allow to better understand the difference in confinement between the two configurations. The extension of the similarity scheme to burning plasmas requires the introduction of a new set of dimensionless parameters directly linked to alpha-particles physics: fixed fusion gain  $Q$ , alpha slowing down time shorter than the energy confinement time and alpha power exceeding the L-H transition threshold. In the case of burning plasmas, alpha particle heating is the dominant heating mechanism, and the plasma state is defined by the fusion reactivity. It is important to notice that two burning plasmas with same  $Q$ , ratio of alpha slowing down time to energy confinement time and alpha power to  $P_{\text{LH}}$  do not necessarily operate at same plasma dimensionless parameters

**Table 3.** Comparison between ITER-similar burning-plasma parameters ( $Q_{\text{fus}} = 10$ ) at  $A = 1.8$  and  $A = 1.45$  obtained using the NSTX (column II and IV) and the ITPA20 scaling (column III). For comparison, column I reports the parameters of a ST ( $Q_{\text{fus}} = 10$ ) plasma calculated with a system code, under different hypothesis [22].

	I	II	III	IV
$R$ (m)	1.51	1.48	1.58	2.31
$a$ (m)	0.84	0.82	0.88	1.59
$A$	1.80	1.80	1.80	1.45
$B/I_p$ (T MA <sup>-1</sup> )	3.73/7.1	3.73/7.29	3.73/7.79	4.27/20
$Q_{\text{fus}}$	10	10	10	10
$P_{\text{fus}}$ (MW)	189	107	118	238
$P_{\text{aux}}$ (MW)	18.9	10.7	11.8	23.8
$H_{y2}$	2.27	3.2	3.5	1.78
$\beta_N$	4	3.8	3.7	1.46
$B$	9.1	9.1	8.7	4.3
$n/n_G$	0.7	0.8	0.8	0.8
$ka/\delta$	2.9/0.5	1.7/0.3	1.7/0.3	1.7/0.3
$q_{\text{cyl}}$	3.55	1.99	1.99	1.99

$\rho^*$ ,  $\beta$ ,  $\nu^*$  safety factor  $q$  but they do operate at the same ion temperature, as a result of the derivation in appendix A. In order to derive the scaling of magnetic field, density and current for similar burning plasma experiments it is necessary to assume the scaling of the confinement time. Three confinement scaling have been used in the derivation, IPB98(y,2), ITPA20 and the NSTX extended scaling at  $A = 1.45$ . The main result of this study consists in the fact that, independently of the scaling, the similarity parameter of burning plasmas, show a much stronger dependency on aspect ratio and magnetic field than the Kadomtsev non-burning plasma similarity parameters. As shown in section 4, this result leads to smaller major radius for ITER similar burning plasmas at different aspect ratio or magnetic field than those derived from non-burning plasma similarity. The parameters of burning plasma experiments similar to ITER but at reduced aspect ratio have been summarized in table 3. For comparison, we have reported in the first column of table 3 (column I) the parameters of a burning plasma experiment derived by A Costley and S McNamara using a system code under different hypothesis.

The second column of table 3 reports the parameters of a ITER similar plasma (in the sense defined in this paper) at  $A = 1.8$  derived using the NSTX scaling, equation (A1.22.1). The  $H$  factor has been found by substituting the ITER parameters in equation (A1.22.1) to obtain the ITER major radius. The third column is derived using the ITPA20 scaling in equation (A1.22.2). Finally, the 4th column has been derived using the NSTX scaling but for an aspect ratio of  $A = 1.45$  and a more conservative  $H_{y2}$  factor ( $H_{y2} = 1.78$ ) and lower beta, which leads to a plasma of major radius 2.3 m producing 238 MW of fusion power.

Comparison between column I and II–III of table 3 shows that the design points found with the method outlined in this paper are not too far from the one obtained using a system

code [22]. However, using the burning plasma similarity argument offers a theory-based framework for the projection of results of existing/under construction/designed tokamak-plasmas to different aspect ratio/magnetic field which increases the level of confidence on the validity of the specific design point.

It is important to notice that the results in this paper on the dimensions of a fusion device are derived from plasma physics constraints related to the hypothesis stated in section 3. However, the concrete feasibility of a fusion reactor is also determined by engineering constraints on the radial build up. For example, constraints related to (a) the dimensions of the neutron shield needed to protect the central solenoid, (b) the space needed for the cooling conduits (either using gas or liquid), (c) the space for the blankets must be considered. The analysis of the above engineering constraints is not included in this paper.

## Data availability statement

No new data were created or analysed in this study.

## Acknowledgments

The authors would like to acknowledge extensive discussions and input by Jack Connor, Alan Costley and Steven McNamara. With their in-depth questions and comments, they greatly helped us to improve the clarity of this article and to comprehend at a deeper level the subtleties of this complicated analysis. We would also like to thank the referees for their great help in improving the readability of the paper.

## Appendix A. Derivation of the scaling for bulk burning-plasma similarity

### A.1. Energy confinement time scaling

In this appendix we will show how the scaling presented in section 3 have been derived from the set of hypotheses which define the similarity between burning plasmas. For this, we shall make use of the ITER IPB(y,2), ITPA20 and the NSTX energy confinement time scaling introduced in section 3. The symbols used in this appendix are the same defined in section 3. The ITER IPB(y,2) scaling can be written in terms of dimensionless variables as:

$$\tau_{\text{IPB}(y,2)} \sim \tau_{\text{B}} \rho^{*-0.7} \beta^{-0.9} \nu^{*-0.01} M^{0.96} A^{-0.73} \text{ka}^{2.3} q^{-3}.$$

$$\tau_{\text{B}} \text{ is the Bohm diffusion time } \sim A^{-2} R^2 B T^{-1} = M \rho^{*-2} B^{-1}.$$

The confinement time ITER IPB(y,2), using the definition of  $\tau_{\text{B}}$ , can then be written in the form:

$$\tau_{\text{IPB}(y,2)} \sim M^{1.96} A^{-0.73} \text{ka}^{2.3} q^{-3} B^{-1} \beta^{-1} \rho^{*-2.7} \beta^{0.1} \nu^{*-0.01}.$$

**Table A1.** Exponents of the confinement time equation (A1.1) for the different scaling.

	IPB(y,2)	ITPA20	NSTX
A	-2.7	-2.24	-3
$\varepsilon_{\text{b}}$	0.1	1.2	0.83
$\varepsilon_{\text{n}}$	-0.01	-0.47	-0.53
$\varepsilon_{\text{q}}$	-3	-0.7	-0.35

In the rest of the analysis, we will use a generalized form of  $\tau_{\text{E}}$ :

$$\tau_{\text{E}} = A_{\tau_{\text{E}}} B^{-1} \beta^{-1} \rho^{*\alpha} \beta^{\varepsilon_{\text{b}}} \nu^{*\varepsilon_{\text{n}}} q^{\varepsilon_{\text{q}}}. \quad (\text{A1.1})$$

For convenience, we have separated the dependence of beta in two terms and the exponent  $\varepsilon_{\text{b}}$  represents the deviation of the scaling on beta from -1.

The parameter  $A_{\tau_{\text{E}}}$  includes a dimensional constant  $C_{\tau}$  and a factor  $H_{\tau}$  to take into account deviations (e.g. increased confinement) from the scaling.

The ITER IPB(y,2) scaling law for H-mode corresponds to indexes in equation (A1.1):

$$\alpha_{\text{H}} = -2.7, \varepsilon_{\text{bH}} = 0.1, \varepsilon_{\text{nH}} = -0.01, \varepsilon_{\text{q}} = -3$$

$$A_{\tau_{\text{EH}}} = H_{y2} C_{\tau y2} M^{1.96} A^{-0.73} \text{ka}^{2.3}. \quad (\text{A1.2})$$

While for the NSTX confinement scaling law we have the following parameters:

$$\alpha_{\text{ST}} = -3, \varepsilon_{\text{bST}} = 0.83, \varepsilon_{\text{nST}} = -0.53, \varepsilon_{\text{qST}} = -0.35$$

$$A_{\tau_{\text{EST}}} = M C_{\tau_{\text{ST}}} H_{\text{ST}}. \quad (\text{A1.3})$$

The ITPA20 scaling law is also used here as derived from a recent analysis of the ITPA global H-mode confinement database, which includes data from NSTX, START and MAST [16].

The ITPA20 scaling law (see [16], equation (8)) has the following expression:

$$\Omega_i \tau_{\text{ITPA20}} = (0.09 \pm 0.14E-6)$$

$$\rho^{*-2.24} \beta^{0.20} \nu^{*-0.47} q_{\text{cyl}}^{-0.70} (1 + \delta)^{0.36}$$

$$\text{ka}^{1.24} A^{1.70} M_{\text{eff}}^{0.53}$$

where  $q_{\text{cyl}} = q^* \text{ka}$ ,  $M_{\text{eff}} = M_i$  effective ion mass,  $\delta$  is the plasma triangularity. Using equation (A1.1), the ITPA20 confinement time is expressed by the following equation:

$$\tau_{\text{ITPA20}} = A_{\tau_{\text{E20}}} B^{-1} \beta^{-1} \rho^{*-2.24} \beta^{1.20} \nu^{*-0.47} q^{-0.70}$$

$$A_{\tau_{\text{E20}}} = C_{\text{ITPA}} H_{\text{ITPA}} (1 + \delta)^{0.36} \text{ka}^{0.54} A^{1.70} M_{\text{eff}}^{1.53}.$$

Table A1 summarizes the values of the exponents for the three different confinement times.

## A.2. Development of the formalism related to the set of burning plasma similarity conditions

### A.2.1. Dimensions of devices similar to ITER at fixed $Q = Q_0$

Using equation (A1.1) and the definition of  $\beta$  (table A1, section 1) the equation  $Q = Q_0$  can be written as:

$$\begin{aligned} Q &= nT\tau_E = \beta B^2 A_{\tau E} B^{-1} \beta^{-1} \rho_*^\alpha \beta^{\epsilon_b} \nu^{*\epsilon_n} q^{\epsilon_q} \\ &= A_{\tau E} B \rho_*^\alpha \beta^{\epsilon_b} \nu^{*\epsilon_n} q^{\epsilon_q} = Q_0. \end{aligned} \quad (\text{A1.4})$$

Note that  $Q$  is linked to the  $Q_{\text{fus}}$  (the fusion gain factor) by the following relations (see [23]):

$$\begin{aligned} Q_{\text{fus}} &= \frac{P_{\text{fus}}}{P_{\text{aux}}} = \frac{\text{fusion power}}{\text{auxiliary heating power}} \\ Q &= Q_0 = nT\tau_E \\ Q_0 &= \frac{1}{K} \left[ \frac{5Q_{\text{fus}}}{5 + Q_{\text{fus}}} \right] \end{aligned}$$

The values of  $Q_{\text{fus}}$  are used in figure 2 rather than the values of  $Q$ .

Inspecting table A1 of this appendix, IPB(y,2) column, we can in first approximation neglect the dependences of the confinement time on  $\beta$  and  $\nu^*$ , since both  $|\epsilon_b|$  and  $|\epsilon_n| \ll 1$ . We can reduce equation (A1.4) to the following expression:

$$Q_0 = A_{\tau E} B \rho_*^\alpha q^{\epsilon_q}. \quad (\text{A1.4.1})$$

The equation (A1.4.1) has the following meaning: burning-plasmas with the same  $Q_0$  can be realized by changing  $\rho^*$  and  $B$  and keeping the other parameters included in  $A_{\tau E}$  and  $q$  constants.

According to the scaling ( $\alpha = -2.7$  for H-mode and  $1/\alpha \approx -1/3$ ):

$$\rho_* \sim B^{1/\alpha} \sim B^{-1/3}. \quad (\text{A1.4.2})$$

Now, recalling the definition of  $\rho^* \sim (TM)^{1/2} B^{-1} R^{-1} A$ , and using equation (A1.4.2), the relation between the major radius and magnetic field is (keeping temperature  $T$  and isotopic composition  $M$  constant, plasma elongation and safety factor  $q$ ):

$$R = \left[ (TM)^{1/2} * (Q_0/A_{\tau E})^{1/3} \right] A B^{-7/5} \sim A^{5/4} B^{-7/5} Q_0^{1/3}. \quad (\text{A1.5})$$

The dependence in equation (A1.5) is only valid for the IPB(y,2) scaling, since expression of  $A_{\tau E}$  from equation (A1.2) is used in equation (A1.5).

According to equation (A1.5), the same  $Q_0$  can be obtained for a smaller major-radius by decreasing the aspect ratio and increasing the magnetic field, while keeping fixed the temperature and ion mass, the value of  $q$  and the elongation. A conventional tokamak operating in the same baseline-scenario regime of ITER ( $Q_{\text{fus}} = 10$ ) can be realized having  $R = 3.48$  m,  $B = 6.5$  T, Aspect ratio  $A = 2.5$  and operating in H-mode at a

plasma current of 12 MA ( $q = 3$ , elongation  $ka = 1.75$ , plasma temperature  $T$  and isotopic composition same as ITER).

Considering an ST device equation (A1.5) becomes (keeping  $q$ , temperature, isotopic composition fixed and neglecting the dependence on the plasma density):

$$R \sim A^{1.5} B^{-0.96} Q_0^{-0.4}. \quad (\text{A1.6})$$

In this case (ST) a device equivalent to ITER ( $Q_{\text{fus}} = 10$ ) can be realized decreasing the major radius to  $R = 4.0$  m, for a magnetic field  $B = 4$  T and aspect ratio  $A = 1.7$ ,  $I_p = 7.4$  MA ( $q = 3$ , elongation  $ka = 1.75$ , plasma temperature  $T$  and isotopic composition same as ITER).

### A.2.2. Analysis of the condition: alpha slowing down time smaller than confinement time

We shall now consider the condition (with  $\Lambda_{\text{SD}}$  a constant  $\ll 1$ ):

$$\tau_{\text{SD}} = \Lambda_{\text{SD}} \tau_E \quad (\text{A1.7})$$

and write both sides of equation (A1.7) as functions of the dimensionless parameters.

The alpha slowing down time is:

$$\tau_{\text{SD}} = A_{\text{SD}} T^{3/2} / n \quad (\text{A1.8})$$

where  $A_{\text{SD}}$  is a dimensional constant. From the definitions of  $\beta$  and  $\nu^*$  we can write the temperature and density as function of these quantities and inserting in equation (A1.7) we obtain:

$$\begin{aligned} A_{\text{SD}} \beta^{-1/6} \nu^{*-5/6} B^{-1/3} A^{5/4} (qR)^{5/6} \\ = \Lambda_{\text{SD}} A_{\tau E} B^{-1} \beta^{-1} \rho_*^\alpha \beta^{\epsilon_b} \nu^{*\epsilon_n}. \end{aligned} \quad (\text{A1.9})$$

Now using equation (A1.4) in equation (A1.9) we obtain the following expression:

$$\frac{\beta}{\nu^*} = \left( \frac{\Lambda_{\text{SD}} Q_0}{A_{\text{SD}}} \right)^{6/5} B^{-2} R^{-1} q^{-1} A^{-3/2} = \varphi. \quad (\text{A1.10})$$

Equation (A1.10) can also be written:

$$\beta = \nu^* \left[ \left( \frac{\Lambda_{\text{SD}} Q_0}{A_{\text{SD}}} \right)^{6/5} B^{-2} R^{-1} q^{-1} A^{-3/2} \right] \equiv \nu^* \varphi. \quad (\text{A1.10.1})$$

### A.2.3. Analysis of the condition: alpha power larger than power threshold for H-mode

We shall now consider the condition:

$$P_\alpha = \Lambda_{\text{th}} P_{\text{LH}} \quad (\text{with } \Lambda_{\text{th}} > 1.5) \quad (\text{A1.11})$$

i.e. alpha power larger than power threshold for H-mode. This condition leads to a decoupling of  $\beta$  and  $\nu^*$ . The power threshold for L-H transition is [24]:

$$P_{\text{LH}} \cup A_{\text{lh}} B^{4/5} n^{3/4} R^2 A^{-1}. \quad (\text{A1.12})$$

The expression for  $P_{\text{LH}}$  can be derived as a function of  $\beta$  and  $\nu^*$ . Inserting the expression obtained in this way, in equation (A1.11) (alpha power higher than the L-H power threshold) we obtain:

$$\begin{aligned} P_{\alpha} &= f_{\alpha} \beta^2 B^4 R^3 A^{-2} = \Lambda_{\text{th}} P_{\text{LH}} \\ &= A_{\text{lh}} \Lambda_{\text{th}} B^{9/5} A^{-11/8} q^{-1/4} R^{7/4} (\nu^* \beta^2)^{1/4}. \end{aligned} \quad (\text{A1.13})$$

$f_{\alpha}$  includes the plasma dilution and some geometrical factors.

From the equation (A1.13) we can deduce a formula linking  $\beta$  and  $\nu^*$ :

$$\beta = \left( \frac{A_{\text{lh}} \Lambda_{\text{th}}}{f_{\alpha}} \right)^{2/3} B^{-22/15} A^{5/12} R^{-5/6} q^{-1/6} \nu^{*1/6} = \chi \nu^{*1/6} \quad (\text{A1.13.1})$$

where the term  $\chi$  is implicitly defined.

Using the equations (A1.13.1) and (A1.10.1) we obtain the expressions for  $\beta$  and  $\nu^*$  in terms of  $\chi$  and  $\varphi$  as follows:

$$\nu^* = \left[ \frac{\chi}{\varphi} \right]^{6/5}; \quad \beta = \varphi^{-1/5} \chi^{6/5}. \quad (\text{A1.13.2})$$

Now combining the last expression for  $\beta$  and using the equation A1.10) we obtain an expression for  $\nu^*$  in terms of the engineering parameters:

$$\nu^* = \left[ \frac{A_{\text{SD}}}{\Lambda_{\text{SD}} Q_0} \right]^{-36/25} * \left[ \frac{A_{\text{lh}} \Lambda_{\text{th}}}{f_{\alpha}} \right]^{1/5} A^{23/10} q R^{1/5} B^{48/25} \quad (\text{A1.14})$$

and a formula for  $\beta$  in terms of engineering parameters as well:

$$\beta = \left[ \frac{A_{\text{SD}}}{\Lambda_{\text{SD}} Q_0} \right]^{6/25} \left[ \frac{A_{\text{lh}} \Lambda_{\text{th}}}{f_{\alpha}} \right]^{1/5} B^{-42/25} A^{4/5} R^{-4/5}. \quad (\text{A1.15})$$

The above expressions are valid for a device operating in H-mode and depend upon: (a) the scaling law assumed for the threshold power for the L-H transition; (b) the conditions equations (A1.4) and (A1.7).

In order to write  $\rho^*$  in terms of engineering parameters, we need to use condition equation (A1.4), i.e. fixed  $Q = Q_0$ :

$$A_{\tau\text{E}} B \rho^{*\alpha} \beta^{\text{eb}} \nu^{*\text{en}} q^{\text{eq}} = Q_0. \quad (\text{A1.16})$$

On the other hand  $\rho^*$  can be expressed using equation (A1.10) and its definition (see table A1),

**Table A2.** Values of the exponents  $\varepsilon_{\varphi}$  and  $\varepsilon_{\chi}$  for IPB(y,2), ITPA20 and NSTX scaling.

	IPB(y,2)	ITPA20	NSTX
$\varepsilon_{\varphi}$	-0.46	-0.05	-0.03
$\varepsilon_{\chi}$	0.11	0.88	0.36

$$\begin{aligned} \rho^* &= \left( \frac{\beta}{\nu^*} \right)^{1/6} M^{1/2} B^{-2/3} R^{-5/6} A^{5/4} q^{1/6} = \varphi^{1/6} \xi \\ &= \left( \frac{\Lambda_{\text{SD}} Q_0}{A_{\text{SD}}} \right)^{1/5} B^{-1} R^{-1} M^{1/2} A. \end{aligned} \quad (\text{A1.17})$$

Using the previous expressions and equation (A1.13.2) we obtain the equation (A1.16) in terms of  $\chi$  and  $\varphi$ :

$$\begin{aligned} \frac{A_{\tau\text{E}} B}{Q_0} \left( \varphi^{\alpha/6} \xi^{\alpha} \right) \left( \varphi^{-1/5} \chi^{6/5} \right)^{\text{eb}} \left( \frac{\chi}{\varphi} \right)^{(6\varepsilon_{\text{n}}/5)} q^{\text{eq}} &= 1 \\ \frac{A_{\tau\text{E}} B}{Q_0} \varphi^{\varepsilon_{\varphi}} \chi^{\varepsilon_{\chi}} q^{\text{eq}} \xi^{\alpha} &= 1 \\ \varepsilon_{\varphi} &= \frac{\alpha}{6} - \frac{\varepsilon_{\text{b}}}{5} - \frac{6\varepsilon_{\text{n}}}{5} \\ \varepsilon_{\chi} &= \frac{6(\varepsilon_{\text{b}} + \varepsilon_{\text{n}})}{5} \end{aligned} \quad (\text{A1.18})$$

From the expressions of the confinement scaling laws (see table A1 of this appendix) we get the values of the exponents  $\varepsilon_{\varphi}$  and  $\varepsilon_{\chi}$  (see table A2).

Now we shall insert in the expressions in equation (A1.18) the definitions of  $\varphi$ ,  $\chi$  and  $\xi$  and the exponents of the various quantities:

$$\begin{aligned} \varphi^{\varepsilon_{\varphi}} &= \left[ \left( \frac{\Lambda_{\text{SD}} Q_0}{A_{\text{SD}}} \right)^{6/5} B^{-2} R^{-1} q^{-1} A^{-3/2} \right]^{\varepsilon_{\varphi}} \\ &= \left( \frac{\Lambda_{\text{SD}} Q_0}{A_{\text{SD}}} \right)^{6\varepsilon_{\varphi}/5} B^{-2\varepsilon_{\varphi}} R^{-\varepsilon_{\varphi}} q^{-\varepsilon_{\varphi}} A^{-3\varepsilon_{\varphi}/2} \end{aligned} \quad (\text{A1.19})$$

$$\begin{aligned} \chi^{\varepsilon_{\chi}} &= \left[ \left( \frac{A_{\text{lh}} \Lambda_{\text{th}}}{f_{\alpha}} \right)^{2/3} B^{-22/15} A^{5/12} R^{-5/6} q^{-1/6} \right]^{\varepsilon_{\chi}} \\ &= \left( \frac{A_{\text{lh}} \Lambda_{\text{th}}}{f_{\alpha}} \right)^{2\varepsilon_{\chi}/3} B^{-22\varepsilon_{\chi}/15} A^{5\varepsilon_{\chi}/12} R^{-5\varepsilon_{\chi}/6} q^{-\varepsilon_{\chi}/6} \end{aligned} \quad (\text{A1.20})$$

$$\begin{aligned} \xi^{\alpha} &= M^{\alpha/2} B^{-2\alpha/3} R^{-5\alpha/6} A^{5\alpha/4} q^{\alpha/6} \\ B - \text{exp} &= 1 - 2\varepsilon_{\varphi} - 22\varepsilon_{\chi}/15 - 2\alpha/3 \\ R - \text{exp} &= -\varepsilon_{\varphi} - 5\varepsilon_{\chi}/6 - 5\alpha/6 \\ A - \text{exp} &= -3\varepsilon_{\varphi}/2 + 5\varepsilon_{\chi}/12 + 5\alpha/4 \\ q - \text{exp} &= -\varepsilon_{\varphi} - \varepsilon_{\chi}/6 + \alpha/6 + \varepsilon_{\text{q}} \\ M - \text{exp} &= \alpha/2 \\ Q_0 - \text{exp} &= 6\varepsilon_{\varphi}/5 - 1. \end{aligned} \quad (\text{A1.21})$$

Using table A3 and equation (A1.18) we obtain the main dependence of the major radius upon the magnetic field for

**Table A3.** Values of the exponents of the variables appearing in equation (A1.18).

	IPB(y,2)	ITPA20	NSTX
<i>B</i> -exp	3.56	1.31	2.53
<i>R</i> -exp	2.63	1.19	2.23
<i>A</i> -exp	-2.64	-2.36	-3.55
<i>M</i> -exp	-1.35	-1.12	-1.50
<i>Q</i> <sub>0</sub> -exp	-1.55	-1.06	-1.04
<i>q</i> -exp	-3.01	-1.17	-0.88

equivalent burning plasma experiments for the ITER IPB(y,2), the NSTX scaling and ITPA20 respectively:

$$R_{\text{ITER}} = C_{\text{ITER}} H_{y2}^{-1/2.62} B^{-1.36} Q_0^{0.59} ka^{-0.88} A^{1.28} M^{-0.23} q^{1.15}$$

$$C_{\text{ITER}} = \left( \frac{\Lambda_{\text{SD}}}{\Lambda_{\text{SD}}} \right)^{-0.55} \left( \frac{\Lambda_{\text{th}} \Lambda_{\text{th}}}{f_{\alpha}} \right)^{0.07} C_{\tau y2} \quad (\text{A1.22})$$

$$R_{\text{ST}} = C_{\text{ST}} H_{\text{ST}}^{-1/2.23} Q_0^{0.46} B^{-1.13} A^{1.59} M^{0.22} q^{0.4}$$

$$C_{\text{ST}} = \left( \frac{\Lambda_{\text{SD}}}{\Lambda_{\text{SD}}} \right)^{-0.04} \left( \frac{\Lambda_{\text{th}} \Lambda_{\text{th}}}{f_{\alpha}} \right)^{0.24} C_{\tau \text{ST}} \quad (\text{A1.22.1})$$

$$R_{\text{ITPA20}} = C_{20} H_{\text{ITPA}}^{-1/1.19} M^{-0.34} A^{0.55} ka^{0.54} B^{-1.02} Q_0^{0.89} q^{0.98} \quad (\text{A1.22.2})$$

Comparing equation (A1.22) with the equations (A1.22.1) and (A1.22.2), we observe that the dependence on the magnetic field is stronger in equation (A1.22) with respect to equations (A1.22.1) and (A1.22.2).

From equation (A1.22) we can derive the scaling parameter for fusion reactors in the hypothesis of ITER IPB(y,2) scaling:

$$S_{\text{FR}} = C'_{\text{ITER}} H_{y2}^{1/2.62} R_{\text{ITER}} B^{1.36} Q_0^{-0.59} ka^{0.88} A^{-1.28} M^{0.23} q^{-1.15}.$$

Using the same method, from the equation (A1.22.1) we can derive the scaling parameter for fusion reactors (1st set of conditions) in the hypothesis of NSTX scaling:

$$S_{\text{ST}} = C'_{\text{ST}} H_{\text{ST}}^{1/2.23} R_{\text{ST}} Q_0^{-0.61} B^{1.13} A^{-1.59} M^{-0.22} q^{-0.4}.$$

The scaling parameter for fusion reactors in the hypothesis of ITPA20 confinement law is (from equation (A1.22.2)):

$$S_{\text{ITPA20}} = C_{20}' H_{\text{ITPA}}^{1/1.19} R_{\text{ITPA20}} M^{0.34} A^{-0.55} ka^{-0.54} B^{1.02} Q_0^{-0.89} q^{-0.98}.$$

#### A.2.4. Scaling laws for plasma parameters and additional heating for STs

From the definition of the dimensionless variables given in section 2.1 expressions can be found relating the plasma parameters to the engineering parameters.

The plasma density for example can be expressed as:

$$n \approx (\beta^2 \nu^*)^{1/3} B^{4/3} R^{-1/3} q^{-1/3} A^{-1/2} \quad (\text{A1.23})$$

$$T \approx \left[ \frac{\beta}{\nu^*} \right]^{1/3} B^{2/3} R^{1/3} q^{1/3} A^{1/2}$$

Inserting in equation (A1.23), the expressions for  $\beta$  and  $\nu^*$  given in equations (A1.14) and (A1.15) we get the following expressions:

$$n \approx (C_{\beta}^2 C_{\nu})^{1/3} B^{1.07} R^{-0.13} A^{0.80}$$

$$T \approx \left[ \frac{C_{\beta}}{C_{\nu}} \right]^{1/3} B^{0.59}$$

$$C_{\nu} = \left[ \frac{\Lambda_{\text{SD}}}{\Lambda_{\text{SD}} Q_0} \right]^{1.44} \left[ \frac{\Lambda_{\text{th}} \Lambda_{\text{th}}}{f_{\alpha}} \right]^{0.20}$$

$$= \left[ \frac{\Lambda_{\text{SD}}}{\Lambda_{\text{SD}}} \right]^{1.44} \left[ \frac{\Lambda_{\text{th}} \Lambda_{\text{th}}}{f_{\alpha}} \right]^{0.20} Q_0^{-1.44}.$$

$$C_{\beta} = \left[ \frac{\Lambda_{\text{SD}}}{\Lambda_{\text{SD}} Q_0} \right]^{0.24} \left[ \frac{\Lambda_{\text{th}} \Lambda_{\text{th}}}{f_{\alpha}} \right]^{0.20}$$

$$= \left[ \frac{\Lambda_{\text{SD}}}{\Lambda_{\text{SD}}} \right]^{0.24} \left[ \frac{\Lambda_{\text{th}} \Lambda_{\text{th}}}{f_{\alpha}} \right]^{0.20} Q_0^{-0.24} \quad (\text{A1.24})$$

From the equation (A1.22.1) we can derive the expression of the scaling of the magnetic field:

$$B \approx C_{\text{ST}}^{0.88} R^{-0.88} A^{1.40} M^{0.20} q^{0.35} Q_0^{0.54}$$

$$I \approx C_{\text{ST}}^{0.88} S R^{0.11} A^{-0.59} M^{0.20} q^{-0.64} Q_0^{0.54} \quad (\text{A1.25})$$

$$C_{\text{ST}} = \left[ \frac{\Lambda_{\text{SD}}}{\Lambda_{\text{SD}}} \right]^{-0.04} \left[ \frac{\Lambda_{\text{th}} \Lambda_{\text{th}}}{f_{\alpha}} \right]^{0.24}$$

Inserting the equation (A1.25) in the equation (A1.24) we get the following scaling laws for the plasma parameters density  $n$  and temperature  $T$ :

$$n \approx C_n R A^{2.20} M^{0.20} q^{0.35} Q_0^{-0.06}$$

$$T \approx C_T R^{-0.52} A^{0.82} M^{0.11} q^{0.2} Q_0^{0.72}$$

$$C_n = \left[ \frac{\Lambda_{\text{SD}f}}{\Lambda_{\text{SD}}} \right]^{0.64} \left[ \frac{\Lambda_{\text{th}} \Lambda_{\text{th}}}{f_{\alpha}} \right]^{0.20}; C_T = \left[ \frac{\Lambda_{\text{SD}}}{\Lambda_{\text{SD}}} \right]^{-0.40} \quad (\text{A1.26})$$

The coefficients  $C_n$  and  $C_T$  are calculated from the equations (A1.25) and (A1.24).

The equations (A1.25) and (A1.26) give the complete set of scalings of plasma parameters for a burning plasma.

**Table A4.** Definition of dimensionless variables.

1.  $\beta \propto \frac{nT}{B^2}$ ,
2.  $\rho^* \propto \frac{(MT)^{1/2}}{aB} = \frac{(MT)^{1/2}}{RB} A$
3.  $q \propto \frac{RB}{A^2 I_p} S = RA^{-2} I_p^{-1} B S$
4.  $\nu^* \propto nRqT^{-2} A^{3/2}$

**Table A5.** Derivation of the relations between  $n$ ,  $T$ ,  $B$ ,  $I_p$  and  $A$ ,  $M$ ,  $R$ .

1.  $\beta \propto \frac{nT}{B^2}$ ,  $\beta$  fixed  $\Rightarrow nT \propto B^2$
2.  $\rho^* \propto \frac{(MT)^{1/2}}{aB} = \frac{(MT)^{1/2}}{RB} A$ ,  $\rho^*$  fixed  $\Rightarrow RB \propto A (MT)^{1/2}$
3.  $q \propto \frac{RB}{A^2 I_p} S = RA^{-2} I_p^{-1} B S$ ,  $q$  fixed  $\Rightarrow I_p \propto RA^{-2} B S$
4.  $\nu^* \propto nRqT^{-2} A^{3/2}$ ,  $\nu^*$  fixed  $\Rightarrow T^2 \propto nRqA^{3/2}$ .

The scaling of the heating power can be obtained from the equation of  $P_{\text{loss}}$ :

$$P_{\text{loss}} = \frac{W_{\text{th}}}{\tau_E} \tag{A1.26}$$

$$P_{\text{loss}} = \frac{nTR^3 A^{-2} ka}{I^{0.54} B^{0.91} P_L^{-0.38} n^{-0.05} R^{2.14}}$$

where the confinement time inserted in the formula for the  $P_{\text{loss}}$  is the NSTX scaling (see equations (A1.1) and (A1.3)). In the equation (A1.26) we use the definition of  $q$  in terms of the shaping factor  $S$  for defining  $I_p$  in terms of  $B$ :

$$q = \frac{5RB}{A^2 I_p} S.$$

Inserting in the equations (A1.26), (A1.24) and (A1.25) for  $n$ ,  $T$ ,  $B$ , we obtain the expression of  $P_{\text{loss}}$ :

$$P_{\text{loss}} \approx (C_{\beta}^2 C_{\nu})^{0.56} (C_{\beta}/C_{\nu})^{0.54} C_{\text{ST}}^{0.37} Q_0^{0.23} R^{-0.08} A^{0.45} M^{0.08} q^{0.15} S^{-0.87} k^{1.61}. \tag{A1.27}$$

The heating power follows from the approximation that  $P_{\text{loss}} \approx P_{\text{aux}}$ .

## Appendix B. Derivation of engineering parameters for non-burning plasmas

In this appendix we will show how the scaling presented in section 2 have been derived from the set of hypotheses which define the similarity between non-burning plasmas. In table A4 the definitions of plasma dimensionless variables are reported for convenience. In the context of the tables A4 and A5 and in the equations (1') and (2'):

The scaling of the engineering parameters with  $A$ ,  $M$ ,  $R$  can be obtained if the dimensionless variables ( $\beta$ ,  $\rho^*$ ,  $\nu^*$ ,  $q$ ) are kept constant. From the definition of the dimensionless variables, the sets of equations in table A5 are derived assuming  $\beta$ ,  $\rho^*$ ,  $\nu^*$ ,  $q = \text{constant}$ :

From equations (1) and (2) we obtain:

$$\frac{nT}{A^2 MT} = \frac{B^2}{R^2 B^2} \Rightarrow \frac{n}{A^2 M} = \frac{1}{R^2}. \tag{1'}$$

Noting that  $q$  is held constant. Substituting the equation for  $n$  equation (1') in equation (4), we get:

$$T^2 = MA^2 R^{-2} RA^{3/2} \Rightarrow T = M^{1/2} R^{-1/2} A^{7/4}. \tag{2'}$$

The scaling for  $B$  and can be derived in analogous way from equations (2) and (3) of table A4.

## ORCID iDs

Michele Romanelli  <https://orcid.org/0000-0003-4897-4843>

Francesco Paolo Orsitto  <https://orcid.org/0000-0002-6644-3635>

## References

- [1] Peng Y K M and Strickler D J 1986 *Nucl. Fusion* **26** 769
- [2] Menard J E *et al* 2012 *Nucl. Fusion* **52** 083015 Menard J E *et al* 2017 *Nucl. Fusion* **57** 102006
- [3] Morris A W *et al* 2017 *IEEE Trans. Plasma Sci.* **46** 1217
- [4] Gryaznevich M *et al* 2017 *Fusion Eng. Des.* **123** 177
- [5] Menard J E *et al* 2019 Development of mission need and preliminary design of a sustained high power density tokamak facility *DPP-CPP initiative proposal* (available at: <https://sites.google.com/pppl.gov/dpp-cpp/home/input-and-feedback>)
- [6] Kadomtsev B B 1975 Tokamak plasma: a complex physical system—IOP Publishing (1992); tokamaks and dimensional analysis *Fiz. Plazmy* **1** 531 1975 *Sov J. Plasma Phys* **1** 295
- [7] Connor J W and Taylor J B 1977 *Nucl. Fusion* **17** 1047
- [8] Luce T C, Petty C C and Cordey J G 2008 *Plasma Phys. Control. Fusion* **50** 043001
- [9] Lackner K 1990 Comments *Plasma Phys. Control. Fusion* **13** 163
- [10] Lackner K 1994 Comments *Plasma Phys. Control. Fusion* **15** 359
- [11] Orsitto F P *et al* 39th EPS/ICPP 2012 Stockholm paper 2.154—Physics driven scaling laws for similarity experiments
- [12] Romanelli M, Romanelli F and Zonca F 2001 On the optimal choice of the dimensionless parameters of burning plasma physics experiments *28th EPS Conf. on Contr. Fusion and Plasma Phys. Funchal (18–22 June 2001)* vol 25A (ECA) pp 697–700
- [13] Freidberg J P *et al* 2015 *Phys. Plasmas* **22** 070901
- [14] ITER Physics Basis NF 39 1999 2208 (<https://iopscience.iop.org/issue/0029-5515/39/12>)
- [15] Buxton P F *et al* 2019 *Plasma Phys. Control. Fusion* **61** 035008
- [16] Verdoolaege G *et al* 2021 The updated global H-mode confinement database: description and analysis *Nucl. Fusion* **61** 076006
- [17] Valovic M *et al* 2005 Energy and particle confinement in MAST *Nucl. Fusion* **45** 942

- [18] Valovic M *et al* 2009 Scaling of H-mode energy confinement with  $I_p$  and BT in the MAST spherical tokamak *Nucl. Fusion* **49** 075016
- [19] Valovic M *et al* 2011 Collisionality and safety factor scalings of H-mode energy transport in the MAST spherical tokamak *Nucl. Fusion* **51** 073045
- [20] Kaye S M *et al* 2006 The role of the aspect ratio and beta in H-mode confinement scalings *Plasma Phys. Control. Fusion* and references therein **48** A429
- [21] Costley A E *et al* 2015 *Nucl. Fusion* **55** 033001
- [22] Costley A E and McNamara S A M 2021 Fusion performance of spherical and conventional tokamaks: implications for compact pilot plants and reactors *Plasma Phys. Control. Fusion* **63** 035005
- [23] Costley A E 2016 On the fusion triple product and fusion power gain of tokamak pilot plants and reactors *Nucl. Fusion* **56** 066003
- [24] Martin Y R *et al* 2008 Power requirement for accessing H-mode in ITER *J. Phys.* **123** 012033